SEMICONDUCTOR-OXIDE NANOCOMPOSITES BASED ON POROUS SEMICONDUCTORS

L. Sirbu[1], V.V. Ursaki[2], I.M. Tiginyanu[1,2], Ks. Dolgaleva[3], and R.W. Boyd[3]

[1]*Technical University of Moldova, 168, Stefan cel Mare str., MD-2004, Chisinau, Republic of Moldova*
[2]*Institute of Applied Physics, Academy of Sciences of Moldova, 5, Academiei str., MD-2028, Chisinau, Republic of Moldova*
[3]*Institute of Optics, University of Rochester, Rochester, New York, 14627, USA*
(Received 12 October 2006)

Abstract

Rare-earth containing oxide nanocomposites are prepared of porous GaP and GaAs templates in a controlled fashion. The initial porous GaP and GaAs networks are replaced by $GaPO_4$ and Ga_2O_3 structures, respectively, during annealing at temperatures from 500 to 900 ^oC. The impregnation of Eu and Er lanthanides from $EuCl_3$:C_2H_5OH and $ErCl_3$:C_2H_5OH solutions results in the formation of lanthanide containing oxide microcrystals finely dispersed into the native oxide matrix. These oxide phases are found to be $EuPO_4$ and $ErPO_4$ in composites obtained on GaP templates, and $EuAsO_4$ and $ErAsO_4$ in composites prepared on GaAs templates. 4f-4f intrashell transitions in Eu^{3+} and Er^{3+} ions assure strong red and green emission from these nanophases.

Introduction

During the recent years there was a considerable interest to the optical properties of rare-earth ion-doped nano-crystals dispersed in a transparent medium as potential optoelectronic materials [1-3]. This issue becomes especially important in connection with the growing interest in the development of random lasers. Random lasers have been realized in a number of material systems, e.g., polymers, liquid crystals and even biological tissues. Recently, Cao reported on a lasing process in highly disordered semiconductor nanostructures [4]. In semiconductor nanostructures, the formation of random laser cavities is attributed to recurrent scattering and interference effects.

A random laser comprises two basic elements: an electromagnetic radiation emitting and amplifying phase and an electromagnetic radiation scattering phase. In some cases the two functions are accomplished by the same phase. The stimulated emission may come either from the near-bandgap electronic effects (exciton-exciton scattering or electron-hole plasma) as in the case of lasers based on ZnO material [4, 5-7], or from the transition metals and rare earth elements doped into the radiation emitting and amplifying phase [8, 9].

Most of the random lasers elaborated to date are based on powders, microspheres, nanocrystallite clusters, polycrystalline films, and disordered organic materials. However, these lasers are not suitable for integration with other optical or electronic functions. Nanocomposite materials prepared on the basis of porous semiconductor templates are more perspective in this regard. Recently, an attempt has been undertaken to dope Eu ions into a porous GaP template [10]. It was supposed that the strong visible emission comes from the Eu^{3+} ions incorporated into the porous GaP host. However, the analysis of the applied techno-

logy suggests that the formation of oxide phases is highly probable; hence, the Eu ions may be incorporated in one of these oxide phases. Moreover, it is well known that rare earth ions are hardly introduced in the tetrahedrally coordinated sites of the III-V host due to their big ion radii [11]. The rare earth ions prefer a coordination number higher than six. It was demonstrated, that the presence of oxygen is an imperative condition for achieving an efficient emission from rare earth ions introduced into the III-V materials [12-15]. The oxygen co-doping leads to the formation of quasi-molecular centers at low concentration of impurity [11-17] and to the segregation of an oxide phase at higher doping [18].

In this paper, we analyze the evolution of the composition and structure of a porous GaP template doped with Eu and Er lanthanides as a function of technological conditions applied to activate the rare earth impurity with the goal to identify the phases responsible for the strong visible emission related to rare earth ions.

1. Experimental details

(100)-oriented n-GaP:S and n-GaAs:S wafers cut from Czochralsky-grown ingots were used for the fabrication of porous GaP layers. The free electron concentration in the as-grown substrates was $(0.3\text{-}0.5)\times10^{18}$ cm^{-3} at 300 K. The anodic etching was carried out in a double-room electrochemical cell as described elsewhere [19]. Eu^{3+} and Er^{3+} ions were incorporated into the por-GaP layer from $EuCl_3$:C_2H_5OH and $ErCl_3$:C_2H_5OH solutions, respectively. Just after infiltration of the solution, the sample is rinsed in ethanol and dried by nitrogen gas. Afterwards, the samples were annealed in a nitrogen flow containing less than 1 % of oxygen by using a halogen lamp heater. The samples were annealed for several minutes to several hours at definite temperatures from the interval 400 to 1000 ^{o}C.

Photoluminescence (PL) was excited by different lines of an Ar^+ SpectraPhysics laser and analyzed through a double spectrometer. The resolution was better than 0.5 meV. The samples were mounted on the cold station of a LTS-22-C-330 cryogenic system.

The morphology and the chemical composition microanalysis of etched samples were studied using a TESCAN scanning electron microscope (SEM) equipped with an Oxford Instruments INCA energy dispersive X-ray (EDX) system.

2. Morphology and composition characterization

The employed porous GaP templates represent porous layers of the depth of 100 mm with pores stretching perpendicular to the sample surface (see Fig. 1a). The rare earth impurity introduced by impregnation into templates was found to be optically activated at annealing temperatures higher than 600 ^{o}C, and as the annealing temperature grows the activation increases. The oxidation of the skeleton walls also starts at temperatures around 600 ^{o}C, and the oxide phase content increases with increasing of the annealing temperature and duration of treatment. At annealing temperature of 900 ^{o}C the porous templates are totally oxidized after 30 min of annealing. For samples with the diameter of pores much larger than the thickness of the porous skeleton walls the annealing results in the formation of a columnar structure as shown in Fig. 1b.

The porous GaAs templates used in this work represent porous layers with a three-dimensional structure containing crossing pores oriented along the <111>B crystallographic directions [20]. The SEM top view of the sample is shown in Fig. 1a. The oxidation of the skeleton walls starts at temperatures under 500 ^{o}C, and the porous template is totally oxidized at annealing temperature of 500 ^{o}C after 30 min of annealing. The morphology of the initial

sample is preserved at annealing temperatures up to 700 °C, it being changed at annealing temperature of 900 °C as shown in Fig. 2b.

The EDX analysis of the oxides demonstrates the formation of stoichiometric $GaPO_4$ and Ga_2O_3 phases in the GaP and GaAs sample as shown in Figs 3 and 4, respectively.

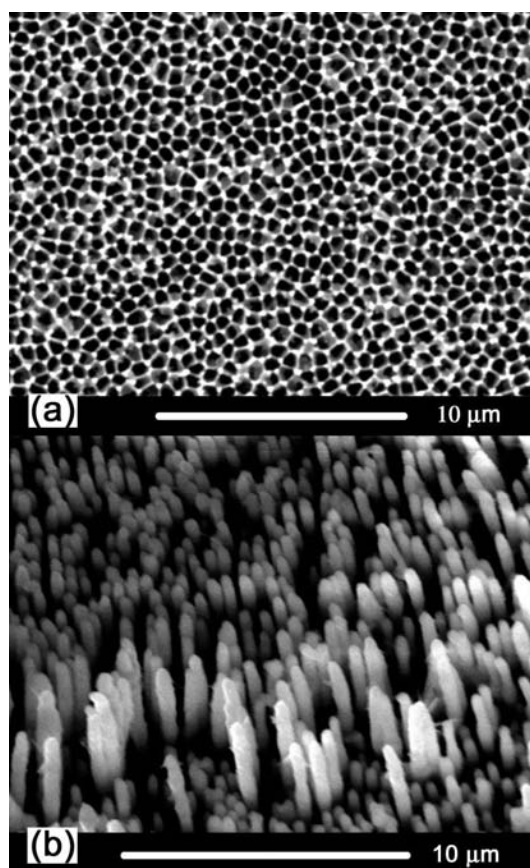

Fig. 1. SEM image of an as-prepared GaP template (a), and the morphology obtained after annealing at 900 °C during 30 min. (b).

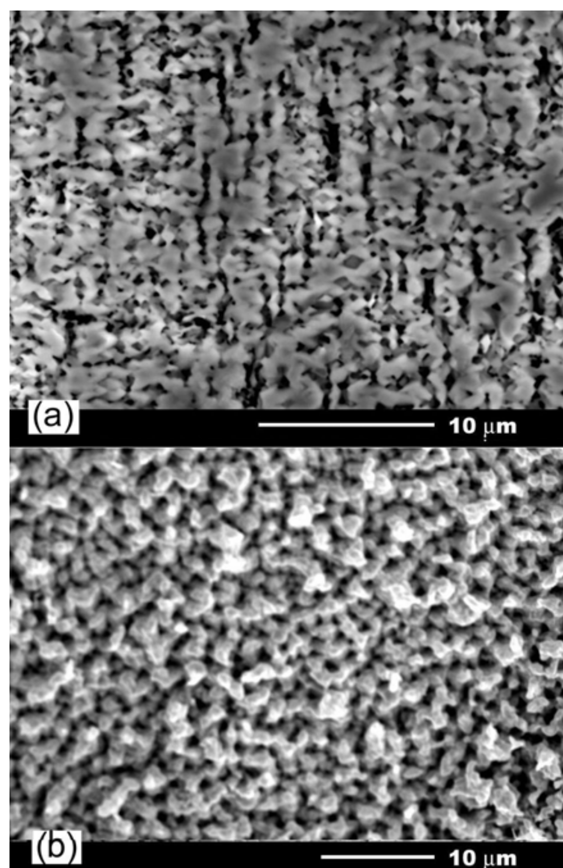

Fig. 2. SEM image of an as-prepared GaAs template (a), and the morphology obtained after annealing at 900 °C during 30 min. (b).

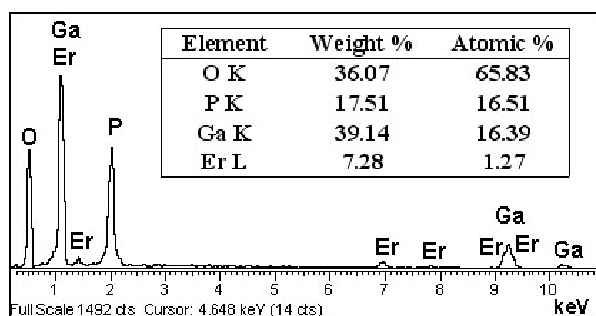

Element	Weight %	Atomic %
O K	36.07	65.83
P K	17.51	16.51
Ga K	39.14	16.39
Er L	7.28	1.27

Fig. 3. EDX analysis of a GaP sample annealed at 900 °C during 30 min.

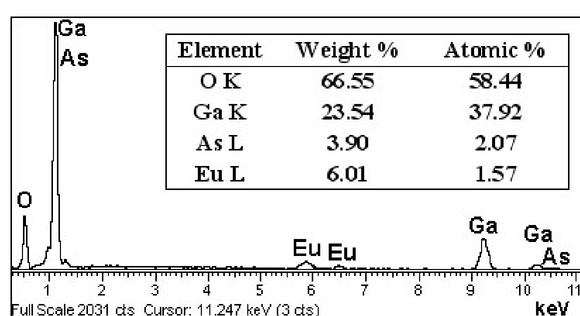

Element	Weight %	Atomic %
O K	66.55	58.44
Ga K	23.54	37.92
As L	3.90	2.07
Eu L	6.01	1.57

Fig. 4. EDX analysis of a GaAs sample annealed at 900 °C during 30 min.

The XRD analysis has shown that apart from low-cristobalite $GaPO_4$ and β-Ga_2O_3 phases, the GaP samples with a high content of lanthanide ions contain monazite $EuPO_4$ and xenotime $ErPO_4$ phases, while the GaAs samples contain xenotime $EuAsO_4$ and $ErAsO_4$ phases.

3. Luminescence characterization

Figures 5 and 6 illustrate the PL spectra of GaP and GaAs samples doped with Er and Eu ions and annealed at 900 °C for 30 minutes. The emission lines corresponding to the Eu^{3+} and Er^{3+} intrashell transitions are well resolved in the PL spectra. Each of the lines corresponding to the respective intrashell transition, as specified in figures, represents actually a multiplet manifold $^{2S+1}L_J$, which results from the Stark spitting due to the crystal electric fields of the host.

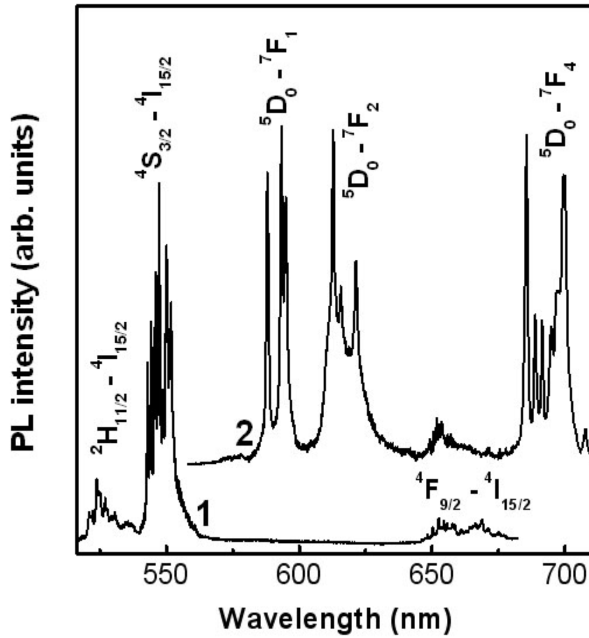

Fig. 5. PL spectra of GaP samples doped with Er (curve 1) and Eu (curve 2) ions.

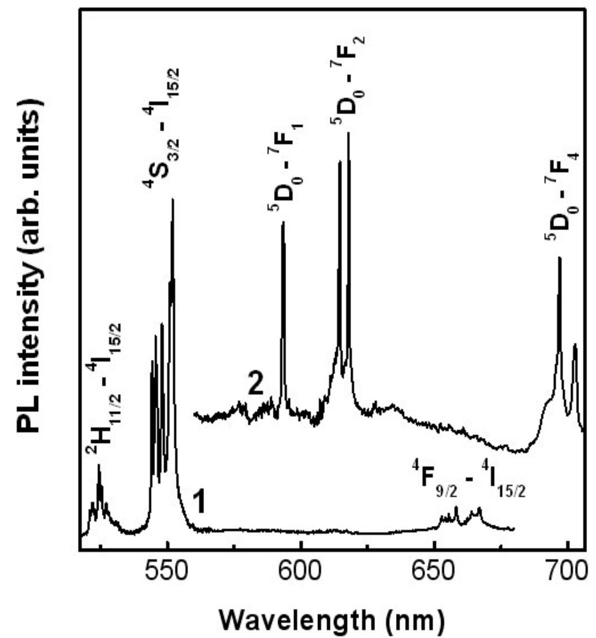

Fig. 6. PL spectra of GaAs samples doped with Er (curve 1) and Eu (curve 2) ions.

Analysis of the luminescence intensity under excitation by different laser lines shows that the highest luminescence intensity from samples doped with Er is observed under excitation by the 488.0 nm laser line (see Fig. 7), while in Eu doped samples this is achieved under the excitation by the 465.8 nm laser line (see Fig. 8). The fact that the quantum energy of these lines corresponds exactly to the $^4F_{7/2} \leftarrow {}^4I_{15/2}$ and $^5D_2 \leftarrow {}^7F_0$ transitions in Er^{3+} and Eu^{3+} ions, respectively, suggests that the excitation occurs via respective transitions, followed by non-radiative relaxation to the lower energy states $^2H_{11/2}$, $^4S_{3/2}$, and $^4F_{9/2}$ in Er^{3+} ions and $^5D_0$ in Eu^{3+} ions. From these states, radiative transitions to the $^4I_{15/2}$ ground state in Er and to $^7F_{1-4}$ states in Eu occur.

The correspondence of the Stark splitting of the ground $^4I_{15/2}$ multiplet manifold of the Er^{3+} ion deduced from Fig. 5 to that previously measured in a xenotime $ErPO_4$ [21] demonstrates that the green emission comes from the Er ions in this host. The spectrum represented by curve 2 in Fig. 5 coincides perfectly with that measured in a monazite $EuPO_4$ [22]. The analysis of spectrum 1 in Fig. 6 suggests that emission comes from Er^{3+} ions incorporated at true D_{2d} sites of the xenotime $ErAsO_4$. Spectrum 2 in Fig. 6 perfectly fits the one previously reported for xenotime $EuAsO_4$ [23].

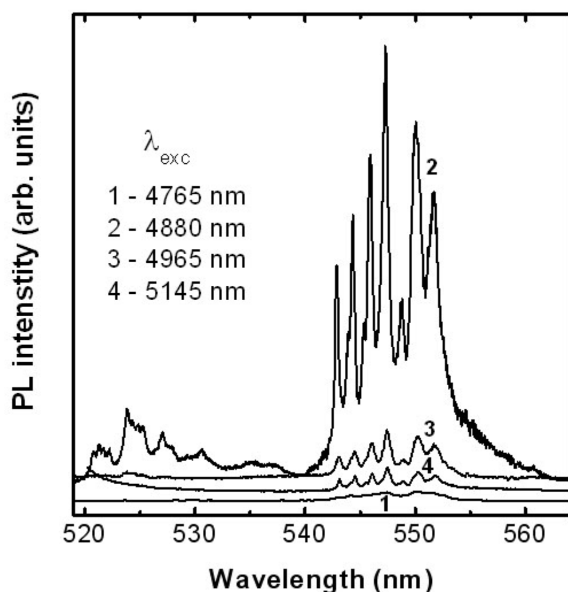

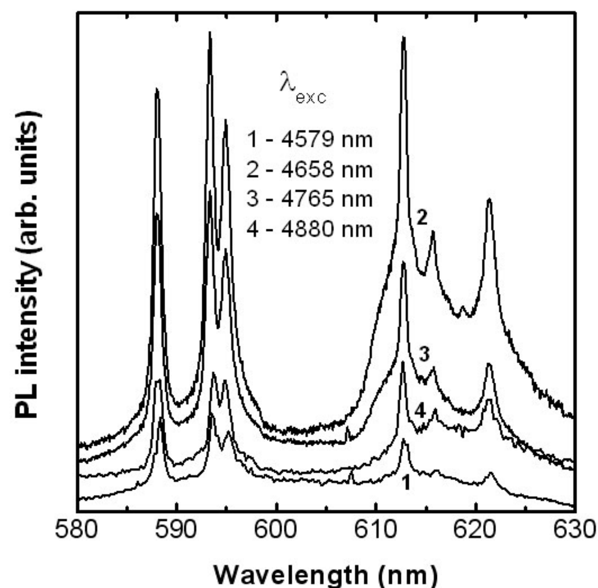

Fig. 7. PL spectra of an Er-doped GaP sample excited with different laser lines.

Fig. 8. PL spectra of an Eu-doped GaP sample excited with different laser lines lines.

Conclusions

The results of this work demonstrate the possibility of preparing in a controlled fashion of a rare-earth-doped semiconductor-oxide nanocomposite of porous GaP and GaAs templates impregnated with rare-earth ions and annealed at different temperatures. Strong red and green emission comes from 4f-4f intrashell transitions in Eu^{3+} and Er^{3+} ions in $EuPO_4$, $ErPO_4$, $EuAsO_4$ and $ErAsO_4$ microcrystals finely dispersed into the composites. These composites are transparent for visible and UV light and may find applications as light emitters for integrated optoelectronic and photonic circuits.

Acknowledgements

This work was supported by US Civilian Research and Development Foundation under grants nos ME2-2527, MR2-995, and MOR2-1033, and Supreme Council for Research and Technological Development of Moldova under grant no 069-a.

References

[1] S.T. Selvan, T. Hayakawa and M. Nagomi, J. Phys. Chem. B, 103, 7064, (1999).
[2] A.P. Barko, L.A. Peyser, R.M. Dickson, A. Mehta, T. Thundat, R. Bhargava and M.D. Barnes, Chem. Phys. Lett., 358, 459, (2002).
[3] V.K. Tikhomirov, D. Furniss, A.B. Seddon, I.M. Reaney, M. Beggiora, M. Ferrari, M. Montagna and R. Rolli, Appl. Phys. Lett., 81, 1937, (2002).
[4] H. Cao, in Progress in Optics, E. Wolf, Ed., 45, North-Holland, Amsterdam, 2003.
[5] X.H. Wu, A.Y. Yamilov, H. Noh, H. Cao, E.W. Seelig and R. Chang, J. Opt. Soc. Am. B, 21, 159, (2004).
[6] S.F. Yu, C. Yuen, S.P. Lau, W.I. Park and G.-C. Yi, Appl. Phys. Lett., 84, 3241, (2004).
[7] H.-C. Hsu, C.-Y. Wu and W.-F. Hsieh, J. Appl. Phys., 97, 064315, (2005).

[8] V.M. Markushev, N.É. Ter-Gabriélyan, Ch.M. Briskina and V.R. Belan, V.F. Zolin, Sov. J. Quantum Electron., 20, 773, (1990).
[9] Ch.M. Briskina, V.M. Markushev and N.E. Ter-Gabrielyan, Quantum Electron., 26, 923, (1996).
[10] H. Elhouichet, S. Daboussi, H. Ajlani, A. Najar, A. Moadhen, M. Oueslati, I.M. Tiginyanu, S. Langa and H. Foll, J. Luminescence, 113, 329, (2005).
[11] N.T. Bagraev and V.V. Romanov, Semiconductors, 39, 1131, (2005).
[12] J.E. Colon, D.W. Elsaesser, Y.K. Yeo, R.L. Hengehold and G.S. Pomrenke, Appl. Phys. Lett., 63, 216, (1993).
[13] A.A. Gippius, V.M. Konnov, V.A. Dravin, N.N. Loiko, I.P. Kazakov and V.V. Ushakov, Semiconductors, 33, 627, (1999).
[14] V.M. Konnov, N.N. Loiko, Yu.G. Sadof'ev, A.S. Trushin and E.I. Makhov, Semiconductors, 36, 1215, (2002).
[15] J. Coutinho, R. Jones, M.J. Shaw, P.R. Briddon and S. Öberg, Appl. Phys. Lett., 84, 1683, (2004).
[16] K. Takahei, A. Taguchi and R.A. Hogg, J. Appl. Phys., 82, 3997, (1997).
[17] M. Yoshida, K. Hiraka, H. Ohta, Y. Fujiwara, A. Koizumi and Y. Takeda, J. Appl. Phys., 96, 4189, (2004).
[18] J.C. Phillips, J. Appl. Phys., 76, 5896, (1994).
[19] S. Langa, I.M. Tiginyanu, J. Carstensen, M. Christophersen and H. Foll, Appl. Phys. Lett., 82, 278, (2003).
[20] H. Foll, S. Langa, J. Carstensen, M. Christophersen and I.M. Tiginyanu, Adv. Mater., 15, 183, (2003).
[21] G.M. Williams, P.C. Becker, N. Edelstein, L.A. Boatner and M.M. Abraham, Phys. Rev. B, 40, 1288, (1989).
[22] J. Dexpert-Ghys, R. Mauricot and M.D. Faucher, J. Luminescence, 69, 203, (1996).
[23] R.L. Cone, M.J.M. Leask, M.G. Robinson and B.E. Watts, J. Phys. C: Solid State Phys., 21, 3361, (1988).